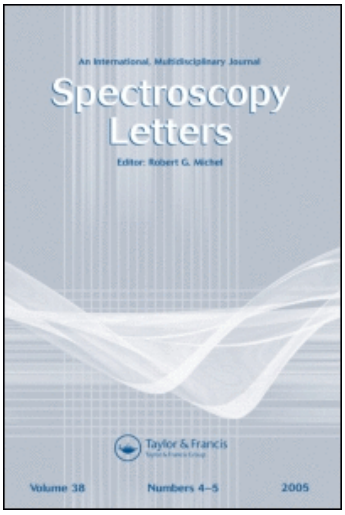

Spectroscopy Letters
Publication details, including instructions for authors and subscription information:
http://www.informaworld.com/smpp/title~content=t713597299

Selected States Magnetic Resonance Spectroscopy (SSMRS): Detection of Paramagnetic Element Dynamics

Czesław J. Lewa[ab]
[a] Institute of Experimental Physics, University of Gdańsk, Gdansk, Poland [b] LRMBM, Faculté de Médedne, Université de Rennes 1, Rennes, France

To cite this Article Lewa, Czesław J.(1998) 'Selected States Magnetic Resonance Spectroscopy (SSMRS): Detection of Paramagnetic Element Dynamics', Spectroscopy Letters, 31: 7, 1569 — 1587
To link to this Article: DOI: 10.1080/00387019808001661
URL: http://dx.doi.org/10.1080/00387019808001661

SPECTROSCOPY LETTERS, 31(7), 1569-1587 (1998)

SELECTED STATES MAGNETIC RESONANCE SPECTROSCOPY (SSMRS): DETECTION OF PARAMAGNETIC ELEMENT DYNAMICS

Key words: magnetic resonance (MR) spectroscopy, Stern-Gerlach effect, spin diffusion, monolevel relaxation times, T_{1m} and T_{2m}, motion studies, magnetic mobility of paramagnetic elements, microviscosity.

Czesław J. Lewa

Institute of Experimental Physics, University of Gdańsk, ul. Wita Stwosza 57, 80-952 Gdańsk, Poland and LRMBM, Faculté de Médecine, Université de Rennes I, Av Prof. L. Bernard, 35043 Rennes, France*

Abstract: *Magnetic resonance (MR) response obtained in a strongly heterogeneous magnetic field with a linear gradient is analysed. It is shown that the employment of strong magnetic field gradients enables the MR spectroscopy to be accomplished in a system with selectively populated energy states (SSMRS). The method can be applied for measuring such physical quantities as the spin diffusion coefficient, D, spin-lattice, T_{1m} and spin-spin, T_{2m}, relaxation times and mobility, ρ_m, of paramagnetic elements in individual Zeeman energy states.*

PACS. 76.60-k – Nuclear magnetic resonance and relaxation
PACS. 76.90+d – Other topics in magnetic resonances and relaxations
PACS. 87.64Hd – EPR and NMR spectroscopy

*) Corresponding address

INTRODUCTION

During the recent decade, marked progress has been made in generating strong magnetic fields with high programmable linear heterogeneity owing to the development in the technology of superconductors and ferromagnetic materials with high magnetic permeability. This raises new, frequently unattainable before, measurement capabilities, for example magnetic resonance (MR) microscopy with the resolution enabling individual paramagnetic ions or nuclei to be detected [1-5]. A possibility of obtaining local gradients of the order of 10^8 *T/m* was considered [4]. In the case of such strong magnetic field gradients, the Stern-Gerlach forces, i.e. the interactions between the gradient G and the magnetic dipole moment μ, should be taken into account. In the fluid environment, this interaction forces the displacement of paramagnetic elements. As a result [6-9], (i) spins with different Zeeman's energies can be separated, (ii) "extreme" population of energy states can be attained [6], (iii) the maser effect can be initiated for spins in individual excited states, (iv) the MR method's sensitivity can be improved by many orders of magnitude [6], (v) the magnetic mobility of paramagnetic elements can be measured.

An analysis of the magnetic resonance response observed in a strongly heterogeneous magnetic field with a linear gradient has been undertaken [6,7] for localized paramagnetic elements. Such a spectroscopy has been termed the Selected States MR Spectroscopy (SSMRS). In 1996, a pulse method to accomplish SSMRS was proposed for spatially distributed paramagnetic elements [8, 9].

In this report, the possibility of measuring such physical quantities as the spin diffusion coefficient D, spin-lattice and spin-spin relaxation times T_{1m} and T_{2m}, respectively, and the mobility ρ, for the individual Zeeman states of these paramagnetic elements by the use of the previously discussed [6-9] changes in the MR parameters evoked by the magnetic field gradient, is presented in more detail.

METHOD

Apart from the spatial differentiation in the MR Larmor frequency, the magnetic field gradient G causes the displacement of paramagnetic elements. This has been known as the Stern-Gerlach (SG) effect which, owing to the spatial quantization with respect to B, leads to the differentiation in the velocity v_m of the motion of paramagnetic elements occupying different Zeeman levels in viscous media [6-9]

$$v_m = \frac{1}{6\pi\eta a_{ef}} \cdot \gamma\hbar m G(t)\cos\Psi \qquad (1)$$

where m is the eigenvalue of the spin operator J_z, Ψ denotes the angle between the direction of the vector of magnetic field B and magnetic field gradient G, γ is the gyromagnetic ratio, $\hbar$ is the Planck constant divided by 2π, a_{ef} is the effective radius of the displaced element, and η is the dynamic viscosity of the medium.

Thus, the direction and velocity of the motion induced by the magnetic field gradient G, assume $(2J + 1)$ discrete and different values. The evolution of the phenomenon in time t_d shorter than the relaxation times T_1 and T_2, proceeds as follows: the initially localized paramagnetic elements, in the neighbouring energy states ($\Delta m = \pm 1$), drive apart from each other with a mean velocity

$$\Delta v_{m,m\pm1} = \frac{\gamma\hbar}{6\pi\eta a_{ef}} G(t) \cdot \cos\Psi \qquad (2)$$

The application of the magnetic field gradient $G(t)$ parallel to the direction of magnetic field B_z (i.e. $\Psi = 0$) enables the Lorentz effect to be neglected. In the pulse SSMRS method [8, 9], quadruple pulse sequence of magnetic field gradient with sinusoidal time dependence G(t) was used. The gradient pulses were separated with pulses with specifically chosen phases. The employment of

such a sequence makes possible the suppression of translational diffusion effects.

Figure 1 shows the time evolution on the example of paramagnetic elements with the spin J = 3/2 at the time of their localization t = 0 (Fig. 1a) and at the moment $t = t_d$ of switching off the time independent field gradient G = const (Fig. 1b). The sequence of RF and displacement $\xi(t)$, of the paramagnetic elements with J = 3/2 induced by: (a) G = const and (b) sinusoidal magnetic field gradient $G = G_o \sin\omega_G t$ of duration t_d (= $2\pi n/\omega_G$ where n is integer) [8,9], are shown in Fig. 2.

Upon switching off a strong and short gradient pulse (i.e. with $t_d << T_1$, T_2), one energy state is only populated in each spin group [6-9]. Such a distribution of energy state population in the individual spin groups opens up new interesting prospects in both theory and experiment.

Paramagnetic elements are subject to different types of intermolecular interactions depending on their properties, as well as on the properties of the environment molecules. Therefore, a shell of the molecules of the medium in the close surroundings of the moving element is involved in its motion. Hence, the effective diameter a_{ef} of the shell depends on the type and intensity of intermolecular interactions. The spins, together with the shells, participate in thermal motion, and their displacement along the SG force direction should be treated as a statistical one. The energy exchange between the spins and the environment results in the change in the orientation of spins. The rate of this exchange is characterized by the spin-spin and spin-lattice relaxation times T_2 and T_1, respectively.

The above analysis [see eq. (2)] implies that for initially localized spins the increase in gradient $G(t)$ is accompanied by the increase in the velocity of moving away of the spins in different energy states. Thus, the possibility of energy exchange between these spin groups decreases and relative effect of other transport processes (such as diffusion and convection) upon spatial spin distribution within each spin group diminishes. As a result, the increase in $G(t)$

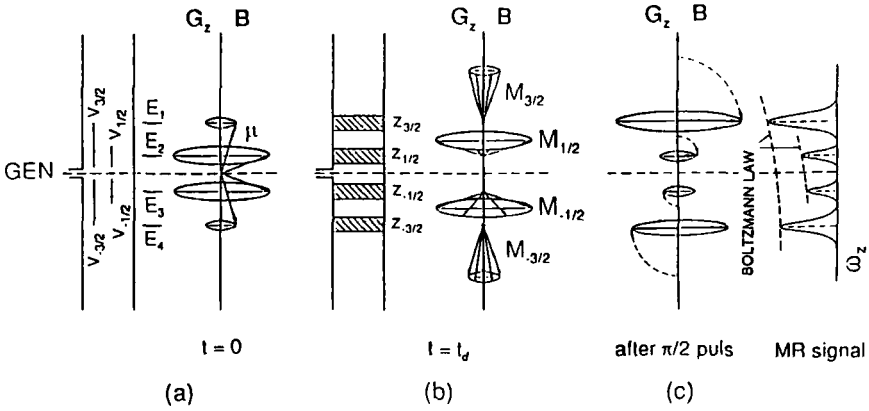

Fig. 1. Illustration of (i) time evolution of the spin position on the z-axis (z // B) on the example of paramagnetic elements with spin $J = 3/2$: (a) at the moment $t = 0$, (b) *at* $t = t_d$, i.e. at the termination of the magnetic field gradient pulse, (ii) the MR response (c) in the form of a spectrum predicted after an RF pulse of $\pi/2$ and FT of FID signal with the assumption of $G_{red} = G$.

will cause: (i) the slowing down of the spin-spin relaxation process, $(T_2)^{-1}$, (ii) the increase in the differences between spin precession on the z-axis along the magnetic field gradient G. Following the application of a proper RF pulse sequence and the gradient of the read-out magnetic field G_{red} [6,7] separate lines corresponding to the individual monoenergetic spin groups occur in the spectrum. Following the application of a proper RF pulse sequence and the gradient of the read-out magnetic field G_{red} (<<G or short duration) [6,7], separate $(2J + 1)$ lines in the frequency domain, corresponding to the individual monoenegetic spin group, occur in the spectrum. The pulse method, following: (a) the initial phase unification for all spin groups, and (b) the use of the proposed G(t) and RF pulse sequence [8,9] differentiating the phase of transverse magnetization components originating from monoenergetic spin groups, and upon the employment of the PSD technique makes possible the obtaining of a spectrum consisting of $(2J + 1)$ lines on the phase scale. In both

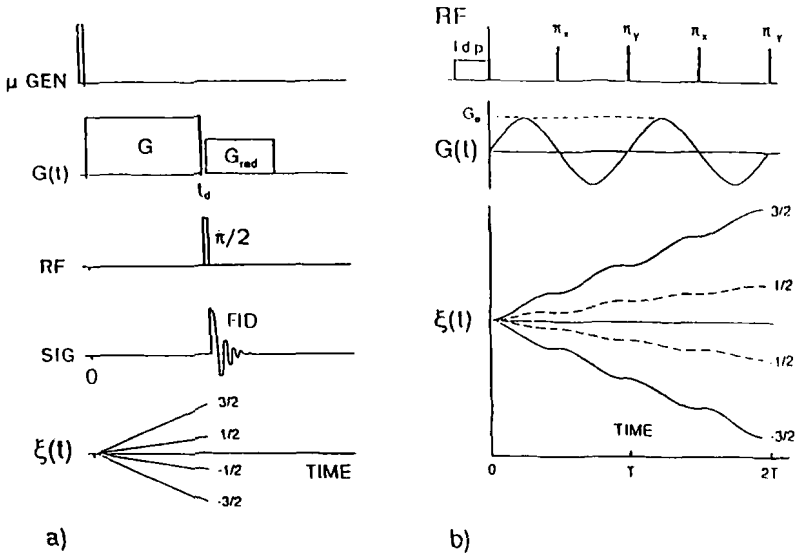

Fig. 2. Time sequence of RF pulses and displacement ξ(t) of the paramagnetic elements with J = 3/2 induced by: (a) $G = const$, and (b) $G(t) = G_o \sin \omega t$.

methods, the intensity of these lines is proportional to the state population (contrary to the classic MR, in which the signal is proportional to the difference in the population of the neighbouring energy states). Figure 3 shows the shape of the predicted MR spectrum for: (a) $G_{red} = G$ following the RF pulse of $\pi/2$ applied at t_d, in the frequency domain and (b) $G(t) = G_o \sin \omega_G t$ with the RF sequence presented in Fig. 2, in the phase domain. The line position on the frequency [6,7] or the phase scale [8,9] enables the displacement of paramagnetic elements, induced by $G(t)$, to be determined, thus making possible the determination of the magnetic mobility of these elements, (iii) the narrowing of spectral lines due to the decrease in the share of stochastic transport processes in the spatial distribution of spins, (iv) the improvement in the monoenergetic character of states in spin groups with different Zeeman energies. This is manifested by the intensification of the maser effect and the increase in the MR

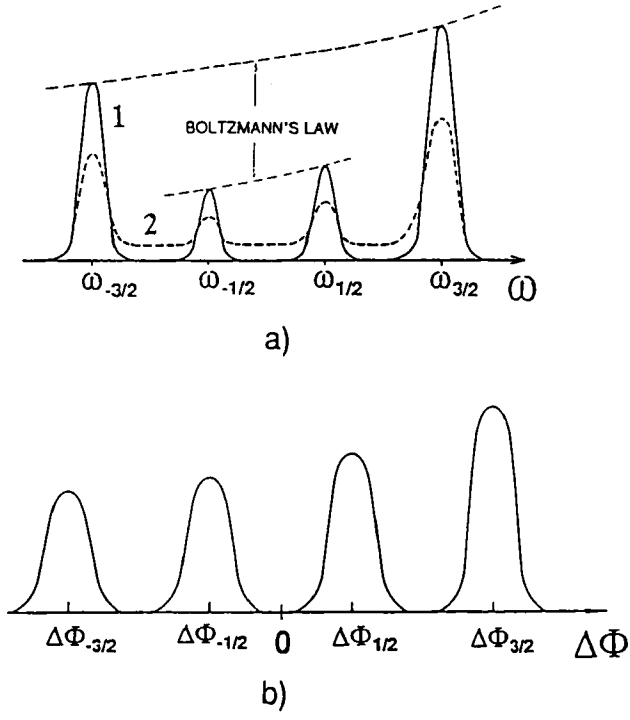

Fig. 3. MR spectrum predicted for: (a) $G = const$ (on the frequency scale), and (b) $G(t) = G_o sin\omega t$ (on the phase scale; divided by m); 1 - for $t_d \rightarrow 0$ and 2 - for t_d comparable with T_{2m}.

signal upon the application of the pulse $\pi/2$, i.e. by the improvement in the MR method sensitivity.

The intensity S_m of spectral lines decreases in time due to the spin-lattice and spin-spin interaction. The observation of the time evolution of the intensity $S_m(t)$, enables the rates of spin-lattice $(T_{1m})^{-1}$, and spin-spin $(T_{2m})^{-1}$, relaxation to be detected for spins from given energy states. It can be concluded that the application of strong magnetic field gradients opens up a possibility to effect the MR spectroscopy for a system with selectively populated Zeeman energy states.

DETECTION OF PARAMAGNETIC ELEMENT DYNAMICS

The realization of the SSMRS methods in practice is possible by employing the time sequence of pulses shown in Fig. 2. In the first method, after time t_d from the moment of switching on the strong magnetic field gradient G, a short (nonselective) RF pulse $\pi/2$ was applied, followed by the read-out gradient G_{red}. Then, the FID signal comprises all components of the spectrum the shape of which is shown in Fig. 3. The employment of phase detection facilitates the differentiation of lines in the spectrum even for small displacements of spins, particularly in the case of the lowest spin numbers (J = ½ or 1) and makes possible the suppression of the diffusion effects [8,9].

In the first approximation, the intensities of individual lines are, proportional to the population of the energy states at the moment $t = 0$ (if processes responsible for the change in the number of elements during the differentiation pulse of the spin-lattice interactions with respect to the spin orientation, are negligible). The line width is primarily determined by the above-mentioned molecular transport processes competing with the flow of initially localized paramagnetic elements, forced by the magnetic field gradient G. The distance between these lines on the frequency scale $\Delta\omega_{m,m\pm1}$, or phase scale $\Delta\Phi_{m,m\pm1}$, depends on gradient G on the z-th component of the magnetic dipole moment μ_z, of the element observed, on time t_d, and viscosity η, of the medium.

In the frequency domain method if the generation of paramagnetic elements is prolonged (e.g. proceeds both prior to and during the pulse of the magnetic field gradient G), the spectral lines observed undergo distortion due to the interference of signals from all the spins generated, thus lowering the resolution of the method. If, however, the start and duration of the generation are precisely determined and its intensity is constant, the description of the response obtained following the RF $\pi/2$ pulse should not present major problems. A short localizing pulse of paramagnetic elements with duration $t_g << t_d$ and a zero lead time t_n, relative to the start of the pulse of magnetic field gradient, is the simplest case.

The measurement of the MR spectrum as a function of the magnetic field gradient value G and its duration t_d, makes possible:

A) The measurement of magnetic mobility, ρ, of paramagnetic elements. According to equation (1), paramagnetic elements move with velocity proportional to the magnetic field gradient G, and the quantum number $|m|$. If, by analogy to the electric mobility of charge carriers, the magnetic mobility of paramagnetic elements ρ_m is defined as the velocity of their displacement in unit magnetic field gradient, v_m/G, one obtains discrete values

$$\rho_m = \frac{\gamma\hbar|m|}{6\pi\eta a_{ef}} \tag{3}$$

In isotropic liquids, the absolute values of the mobility should be identical for states $+m$ and $-m$, hence, being given by $|m|$. The mobility characteristics of a given type of paramagnetic elements in a given medium can be defined by the quantity v_m/mG independent of the energy state of the spins. If the gradient G is constant along the z-direction, the motion of spins along the G-direction is uniform for all spin groups, proceeding with a velocity characteristic of each energy state. Accordingly, the position of lines on the frequency or phase scale, relative to the centre of the spectrum, is a linear function of the displacement of paramagnetic elements at time t_d.

Hence, the mobility of paramagnetic elements in individual energy states is

$$\rho_m = \frac{\Delta\omega_m}{G \cdot G_{red} t_d} \tag{4}$$

And their characteristic mobility $\eta_{ch} = \eta_m/m$.

The measurement of ρ_m and the distribution of ρ_{ch} as a function of m provides information on the local magnetic anisotropy or heterogeneity of the medium.

The comparison of equations (3) and (4) enables the microscopic parameter ηa_{ef} to be determined.

$$\eta \cdot a_{ef} = \frac{\gamma \hbar m \vec{G} \cdot \vec{G}_{red} t}{6\pi \Delta \omega_m} \tag{5}$$

The direct measurement of ηa_{ef} may be of fundamental significance for the recognition of microviscosity of liquids. Although the definition of this quantity results from simple assumptions, the capability of its measurement creates one of few chances for the experimental verification of the theoretical definitions of microviscosity.

B) The measurement of translational diffusion coefficient D_t of paramagnetic elements. For direct measurement of D_t, the velocity of moving away of paramagnetic elements should be incomparably higher than the rates of relaxation and other transport processes such as convection, charge carriers flow etc. The fulfilment of this condition necessitates the application of an extremely strong magnetic field gradient G. One may presume, based on the Einstein relation, that the widening of a single line in the spectrum $\Delta\delta$, (Fig. 3) is proportional to the square root of the diffusional displacement of the spins observed, i.e.

$$\Delta\delta = \alpha\sqrt{6Dt_d} \tag{6}$$

where α is the constant of proportionality.

C) The measurement of relaxation time T_{1m} for individual energy states. The change in the spectral line intensity as a function of t_d makes possible the determination of the spin-lattice relaxation times T_{1m}, for spins from individual energy states. After time t_d, as a result of energy exchange with the lattice, a part

of the spins from states populated at time $t_d \rightarrow 0$ will pass to the states with the zero initial population (cf. Fig. 4). Each time after the energy exchange, the spins change their velocity to conform to their new orientation relative to the magnetic field gradient. Following the energy exchange (when neglecting the diffusion process) a small change in the spin position can only be found in any spin groups in the primary states. This means that in the first approximation their effect upon the intensity of lines originating from the spins remaining in the primary energy states is negligible. The signal from the spins in new energy states for $t_d > 0$ does not coincide with the centre of signals from spins at the moment t_d. It is manifested in the spectrum in the form of one-side broad wings for the terminal lines (in the case shown in Fig. 1c and Fig. 3, the signal originating from the spins in states $m = 3/2$ and $m = -3/2$ appears between lines $S_{3/2} - S_{1/2}$ and $S_{-1/2} - S_{-3/2}$, respectively, since as a result of energy exchange with the lattice, these spins cannot exceed the absolute value of the velocity of their movement before the energy exchange; they can only slow down or change the direction of the motion) and broad two-sided wings for the central lines (in the case shown in Fig. 1c, the signal from the spins in states m = ½ and m = - ½ appears between all the lines, since these spins can be accelerated or change the direction of the motion). Figure 3a illustrates the predicted shape of the spectrum for $t_d \rightarrow 0$ (curve 1) and t_d comparable with T_{1m} (curve 2). In a first approximation, the dependence of the line intensity (calculated from the base corresponding to $t_d = 0$) upon t_d can be described as

$$S_m(t_d) = S_m(0) \cdot \exp\left[-\frac{t_d}{T_{1m}}\right] \tag{7}$$

where $S_m(0)$ is the intensity of the line originating from the spins in a state given by the magnetic quantum number, m, for $t_d \rightarrow 0$.

The measurement of T_{1m} for the individual energy states can be of essential importance in the aspect of fundamental research, for strongly

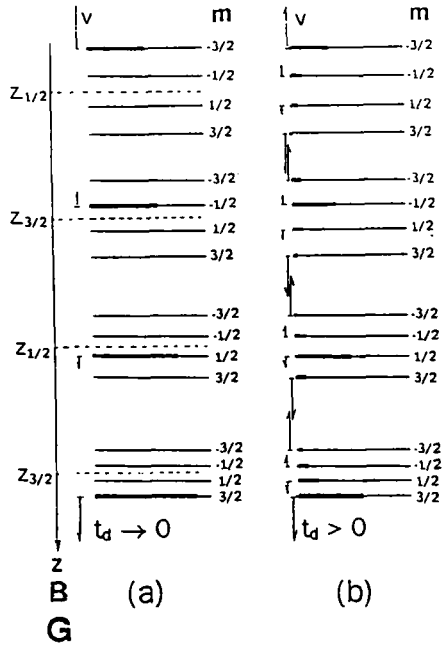

Fig. 4. Zeeman energy states distribution and population achieved upon termination of the G pulse for two value of t_d: (a) $t_d << T_{2m}$, (b) t_d comparable with T_{2m} assuming that the condition $G \cdot t_d = const$ is satisfied. Arrows indicate the direction of the relative motion of spins forced by SG (for B //G).

heterogeneous media with anisotropic properties, e.g. for ferromagnetic liquids, liquid crystals in the areas of phase transitions, solutions containing macromolecules with polar groups or displaying paramagnetic properties, as well as for paramagnetic elements which are strongly anisotropic (e.g. with anisotropy of reorientation) and adsorb anisotropically the molecules of the medium or comprise hydrophobic and/or hydrophilic groups etc.

D) The measurement of spin-spin relaxation time T_{2m} for different energy states. The application of an extremely strong pulse of magnetic field gradient G, enabling spin groups in different energy states to be distinctly separated in time

t_d short enough to neglect the effects evoked by diffusion and spin-lattice relaxation, creates favourable conditions for measuring the spin-spin relaxation time T_{2m}, for individual energy states, e.g. by the CPMG method. Figure 4 shows the energy state distribution established after the termination of a strong pulse of the magnetic field gradient G for two values of t_d: $t_d \ll T_{2m}$ (part a) and t_d comparable with T_{2m} (part b), satisfying the condition $G \cdot t_d = const$, when disregarding the relaxation T_1 and diffusion processes. The application of the pulse sequence $\pi/2\text{-}\tau\text{-}\pi\text{-}2\tau\text{-}\pi\ldots$ upon termination of the magnetic field gradient pulse enables time T_{2m} to be determined in a homogeneous magnetic field B, yet, under conditions unfavourable for direct energy exchange between the spins occupying different energy levels. The measurement of this quantity as a function of the magnitude of the separation of spins in different energy states can be useful to verify the mechanisms of the spin-spin relaxation and to determine the concentration of the spatial distribution of paramagnetic elements other than those initially localized before starting the experiment (at $t \leq 0$).

ACCURACY EVALUATION

The relative resolution of the method in the frequency domain is given by the relation

$$\frac{\Delta\omega}{\omega} = \frac{\gamma\hbar G \cdot G_{red} t_d}{6\pi\eta a_{ef} B} \cos\Psi \tag{8}$$

where $\Delta\omega$ is the MR frequency difference for the neighbouring energy states.

The relative width of the spectral line is, in a first approximation, determined by the relative rate of diffusional displacements related to the displacements forced by the magnetic field gradient

$$\frac{\Delta\omega_D}{\Delta\omega} \propto \frac{6\pi\eta a_{ef}\sqrt{6D/t_d}}{\gamma\hbar G\cos\Psi} \tag{9}$$

Table I summarizes the values of magnetic dipole moments μ, (column 2), quantum numbers J, (column 3) [10,11], velocity of moving away of spins Δv, and the differences $\Delta\nu$, in the MR frequencies in the neighbouring energy states for several paramagnetic elements in the air and water, assuming $\eta = 1cP$ for water and $\eta = 182\ \mu P$ for air [11], $a_{ef} = 10\ \AA$ and $G_{red} = G = 10^2\ T/m$ and $10^6\ T/m$.

DISCUSSION

Getting an insight into the dynamics of the motion of paramagnetic elements and the related phenomena is important for fundamental research, as well as for many processes occurring in natural systems. For example, the dynamics of the migration of paramagnetic or ferromagnetic elements (e.g. metal ions and free radicals or ferritine) in a cell is of essential importance for numerous biological processes. There are many reports on the significance of paramagnetic elements, in particular of metal ions such as Mn^{2+}, Cu^{2+}, Fe^{3+}, Fe^{2+}, Co^{2+}, Ni^{2+} or Zn^{2+}, electrophilic radicals [12] and ferritine [13], and their transport in a cell for the evolution of pathological changes such as the ageing process and cellular transformations (e.g. neoplastic processes) [14-16]. Marked differentiation in paramagnetic ion concentration in pathological and healthy tissues was indicated [17-20]. Biochemical reactions, in which free radicals play a significant role, are also important in many physiological functions.

Time and temperature change observed *ex vivo* in relaxation times T_1 and T_2 [21-25] of some tissues (e.g. liver and pancreas) are related with a marked content of manganese ions in the nucleus and mitochondria and with their migration through membranes [23].

The explanation of the transport of paramagnetic elements is also important for the determination of the time dependence of the distribution of contrast agents in magnetic resonance imaging (MRI) in diagnostics [26-28], in magnetic resonance spectroscopy (MRS) of biofluids [28], in the monitoring of generation and disappearance of free radicals in metabolic pathways [13-15], in

Table 1.

The velocity of moving away paramagnetic elements and relative line frequency differences for different monoenergetic spin groups in the MR spectrum (cf. Fig. 3a), assuming a_{ef} = 10 Å and G_{red} = G. The viscosity of the medium and magnetic dipole moments were taken from the literature [10,11].

			$G = 10^2$ T/m				$G = 10^6$ T/m			
			WATE		AIR		WATE R		AIR	
ELE-MENTS	μ/μ'	J	$\Delta\nu$ [Å/s]	$\Delta\nu$ [kHz]	$\Delta\nu$ [nm/s]	$\Delta\nu$ [MHz]	$\Delta\nu$ [μ/s]	$\Delta\nu$ [MHz]	$\Delta\nu$ [μ/s]	$\Delta\nu$ [MHz]
Mn^{2+}	5.9	5/2	1.2	2.49	6.7	0.14	1.2	2.49	67	139.0
Fe^{3+}	5.9	½	5.8	60.19	34.0	3.53	5.8	60.19	34	3528
Fe^{2+}	5.0	2	1.2	2.64	7.1	0.16	1.2	2.64	71	156.1
Co^{2+}	4.4	3/2	1.4	3.61	8.3	0.21	1.4	3.61	83	214.1
Cu^{2+}	1.8	1/2	1.8	5.70	10.0	0.32	1.8	5.70	100	316.6
1H	2.783	1/2	0.09	0.002	0.50	0.00013	0.09	0.02	5.0	1.30
19F	2.629	1/2	0.08	0.002	0.47	0.00014	0.08	0.02	4.7	1.40
31P	1.132	1/2	0.03	0.0003	0.20	0.00002	0.03	0.003	2.0	0.20

For ions, μ' is the Bohr magneton (= $9.2740154 \times 10^{-24}$ JT^{-1})
For nuclei, μ' is the nuclear magneton (= $5.0507866 \times 10^{-27}$ JT^{-1})

radiotherapy or detection of the effects of ionising irradiation [29,30], and for the needs of the dynamically developing techniques of electron spin resonance imaging (ESRI) [19,31]. It can also be useful in the evaluation of thermodynamic and kinetic stability of free radicals, their stabilization and destabilization, in the determination of the constants of reaction rates etc.

On the other hand, there are many frequently contradictory reports on either invasive [16,32] or therapeutic [33,34] effect of the magnetic field. Some of them imply that beneficial therapeutic results are achieved when applying a time-variable field with a selected frequency and marked heterogeneity [32-34]. So far, there has been no unequivocal interpretation of both harmful and favourable effect of the electromagnetic field. It is possible that the results obtained in this field depend on the activation of certain groups of para- or/and ferromagnetic elements by their intensified mobility inside the cell, forced by the external electromagnetic field.

CONCLUSION

A proposition to apply the MR spectroscopy in a strongly heterogeneous magnetic field with a linear gradient has been presented for paramagnetic elements under condition of pulsed localization (generated, injected or magnetically localized) in a liquid medium. The interaction of the Stern-Gerlach type result in the spatial separation of spin groups in different energy states, thus making possible the observation of a spectrum with resonance lines corresponding to the individual spin groups in different energy states. The intensity of these lines is proportional to the population of the states, as opposed to the classic MR methods with the intensity proportional to the difference in the population of the neighbouring states. Therefore, the sensitivity of this method should be higher by many orders of magnitude than that attained in the classic MR techniques. The investigation of the dependence of the width, intensity and separation of individual spectral lines upon the duration, t_d, of the pulse of a strong magnetic field gradient, G, affords possibilities of detecting parameters such as translational spin diffusion coefficient, D, spin-lattice and spin-spin relaxation times, T_{1m} and T_{2m}, respectively, and the mobility of spins in individual energy states, as well as their characteristic mobility and the microviscosity of the medium. The employment of strong magnetic field gradient pulses creates possibility for the application of the MR spectroscopy to systems with selectively populated energy states. One can presume that the combination of the method proposed [4-10] with the MR microscopy [1-5] will in near future provide chances for detecting the dynamics of the motion of paramagnetic elements in microspaces with dimensions of the order of those of cells or their constituents.

This research was supported by the KBN grant No. 2 PO3B 148 12.

REFERENCES

1. J.A. Sidles, Noninductive detection of single-proton magnetic resonance, *Appl. Phys. Lett.*, 1991; 58: 2854-2856

2. J.A. Sidles, Folden Stern-Gerlach experiment as a means for detecting nuclear magnetic resonance in individual nuclei, *Phys. Rev. Lett.*, 1992; 68: 1124-1127

3. G.J. Moore, P.C. Hammel and M.L. Roukes, Design of highly sensitive magnetic resonance force microscope, *13th Ann. Meet. SMRM*, San Francisco 1994, p. 753

4. D. Rugar, C.S. Yannoni and J.A. Sidles, Mechanical detection of magnetic resonance, *Nature*, 1992; 360: 563-566

5. G.J. Moore, J.A. Hanlon, R. Pryputniewicz, B. Lamartine M. Hawley, J.C. Solem, S. Singer, J.J. Jamer, S. Penttila and L.O. Sillerud, NMR force microscopy: Development of polarized samples for nuclear detection, *12th Ann. Meet. SMRM*, New York 1993, p.299

6. C.J. Lewa, Selected states magnetic resonance spectroscopy (SSMRS), *J. Magn. Reson. Analysis*, 1996; 2: 110-112

7. C.J. Lewa, SSMRS by EMRS method application, *VII Cong. GRAMM*, Sant-Malo 1996, (LRMBM, Univ. Rennes 1, France)

8. C.J. Lewa, J.D. de Certaines, Selected states magnetic-resonance spectroscopy: A potential method for huge improvement in sensitivity, *Europhys. Lett.*, 1996; 35: 713-718

9. C.J. Lewa, Magnetic field gradient resonance spectroscopy (MGRS), *14th Ann. Meet. ESMRMB*, Brusseles 1997

10. *Handbook of electron spin resonance. Data sources, computer technology, relaxation, and ENDOR*, C.P. Poole, H.A. Farach (Eds.) AIP Press, New York 1994

11. *American Institute of Physics Handbook*, D.E. Gray, (Ed.), McGraw-Hill Book Company, Inc. New York, Toronto, London 1963

12. J. Fossey, D. Lefort and J. Sorbay, *Les radicaux libres en chimie organique*, Masson, Paris 1993

13. A. Stahl and J. Ageneray, *Exploration biochimique du fer et des cellules du sang, In Biochimie clinique*, t. 3, P. Metais (Ed.) SIMEP 1988

14. *Essential and toxic trace elements in human health and disease*, A.S. Prasad (Ed.), New York, NY: Arliss 1988

15. *Biochemistry of the essential ultratrace elements*, E. Frieden (Ed.), Plenum New York, NY 1984

16. R.L. Brent, W.E. Gordon, W.R. Bennett and D.A. Beckman, Reproductive and teratologic effects of electromagnetic fields, *Reproductive Toxicology*, 1993; 7: 535-580

17. W. Negendank, T. Corbett, M. Crowley and C. Kellogg, Evidence for contribution of paramagnetic ions to water proton spin-lattice relaxation in normal and malignant mouse tissues, *Magn. Reson. Med.*, 1991; 18: 280-293

18. J.H. Schumacher, E.R. Matys, J.H. Clorius, H. Hauser, H. Wesch and W. Maier-Borst, Contribution to paramagnetic trace element to the spin-lattice relaxation time in the liver, *Invest. Radiol.*, 1985; 20: 601-608

19. H. Sakurai, M. Nishida, T. Yoshimura, J. Takada and M. Koyama, Partition of bivalent and total manganese in organs and subcellular organelles of $MnCl_2$ – treated rats studied by ESR and neutron activation analysis, *Biochem. Biophys. Acta*, 1985; 841: 208-214

20. Ys. Kang and J.C. Gore, Studies of tissue NMR relaxation enhancement by manganese dose and time dependence, *Invest. Radiol.*, 1984; 19: 399-407

21. C.J. Lewa and Z. Majewska, Temperature relationships of proton spin-lattice relaxation time T_1 in biological tissues, *Bull. Cancer*, 1980; 67: 525-530

22. C.J. Lewa and M. Lewa, Temperature dependence of 1H NMR relaxation T2 for intact and neoplastic plant tissues, *J. Magn. Res.*, 1990; 89: 219-226

23. Y. Baba, M.M. Lerch, D.D. Stark, A. Tanimoto, B.P. Kreft, L. Zhao, A.K. Saluja and M. Takahashi, Time after excision and temperature alter ex vivo tissue relaxation time measurements, *J. Magn. Res. Imaging*, 1994; 4: 647-651

24. E. Moser, E. Wunklmayr, P. Holzmuller and M. Krssak, Temperature and pH-dependence of proton relaxation rates in rat tissue, *Magn. Res. Imaging*, 1995; 13:429-440

25. P.A. Bottomley, T.H. Foster, R.E. Argersinger and L.M. Pfeifer, A review of normal tissue hydrogen NMR relaxation times and relaxation mechanism from 1-100 MHz, dependence on tissue type, NMR frequency, temperature, species, excision, and age, *Med. Phys.*, 1984; 11: 425-448

26. *Contrast agents for MRI tissue characterization: basic principles and research methodology*, J.D. de Certaines and F. Podo (Eds) Europ. Comm., Luxembourg 1988

27. *Magnetic resonance imaging*, D.D. Stark and W.G. Brandley (Eds), Mesby-Year Book, Inc., St Louis 1992

28. *Magnetic resonance spectroscopy in biology and medicine*, J.D. de Certaines, W.M.M.J. Bovee and F. Podo, Pergamon Press, Oxford, New York, Seul, Tokyo 1992

29. C. Von Sonntag, *Chemical basis of radiation biology*, Taylor and Francis, London, New York, Philadelphia 1987

30. T.L. Walden and N.K. Farzaneh, *Biochemistry of ionizing radiation*, Raven Press, New York 1990

31. M. Ikeya, Scanning and computer thomography – ESR microscopy, and L.J. Berliner, Application of EPR imaging to materials agriculture and medicine. In *Magnetic resonance microscopy; Methods and applications in materials science, agriculture and biomedicine*, B. Blümich and W. Kuhn (Eds), VCH Weiheim, New York, Basel, Cambridge 1992

32. W.R. Hendee and J.C. Boteler, The question of health effects from exposure to electromagnetic fields, *Health Phys.*, 1994; 66: 127-136

33. A. Bellossi, Effect of a 12 Hz and a 460 Hz pulsed magnetic field on the weight of AKR mice, *Biotherapy*, 1992; 4: 277-283

34. A. Bellossi, Effect of a pulsed magnetic field on AKR female mice offspring. *Panminerva Med.*, 1992; 34: 40-44

Date Received: May 27, 1998
Date Accepted: June 29, 1998